DOI: 10.13009/EUCASS2017-81

Physical mechanisms of increased heat flux zone appearance and laminar-turbulent transition in the boundary layer on blunted delta wings at high freestream velocities

V.I. Shalaev, S.V. Alexandrov, and A.V. Vaganov
Moscow Institute of Physics and Technology (State University)
Central Aaerohydrodynamic Institute
Russia, Zhukovsky, 140180

Abstract

On the base of experimental investigations and numerical solutions of Navier-Stokes equations processes of quasistreamwise vortex formation and their interactions with the hypersonic boundary layer on the delta wing with blunted leading edges are analyzed. New physical mechanisms of the appearance of abnormal zones with high heat fluxes and the early laminar turbulent transition are studied. These phenomena were observed in many high-speed wind tunnel experiments however their understanding and explanation became possible only using the detailed analysis of high resolution numerical modelling results. ANSYS CFX code (the DAFE MIPT license) on the grid with 50 million nodes was used for the numerical modelling. The numerical method was verified by comparison calculated heat flux distributions on the wing surface with experimental data.

1. Introduction

A study of 3D hypersonic flows of a viscous thermo-conducting gas is very actual problem of the today aerodynamics and has a significant interest for applications to developing a new generation of high speed flying vehicles. Investigations of these problems collide with difficulties due to confined experimental methods. Some progress was reached using asymptotic methods and the boundary layer theory [1]. In these frameworks, basic controlling parameters for this flow class were revealed, effects viscous-inviscid interaction, the disturbances propagation, the separation appearance in the laminar boundary layer were studied; self-similar solutions were constructed and heat exchange problems were considered. In the same time, a set of phenomena observed in experiments still didn't get an adequate explanation up to date.

Found in experiments [2 – 8] zones of abnormal high heat fluxes on the windward surface of delta wings with blunted leading edges and other similar configurations are appertained to such phenomena. Effects to these anomalies of the Mach number, the bluntness radius and the angle of attack were investigated in details in TsAGI wind tunnels T-117 and UT-1M. In the process of these investigations, the presence of the early laminar-turbulent transition was found, which can't be explained in frameworks of usual conceptions [2 – 4, 8]. In all these works, surface phenomena were studied mainly using soot-oil or thermo-indicator coatings; plane shadow flow patterns didn't allow clarifying a detailed spatial flow structure in order to relate it with observed effects. Thermoanemometer measurements of developing disturbances didn't clarify also the problem essence [9].

The numerical modeling of the considered flow was conducted on the base of parabolized Navier-Stokes equations [9], Euler equations [10] and full Navier-Stokes equations [11, 12]. In the work [9], the high heat flux spot observed on the wing leading edge near the nose was related to the flow reconstruction from the explosive type near the apex to the regime of the flow around the swept leading edge. The hypothesis was proposed about the hanging shock wave appearance due to the flow turn. The S-shaped head shock wave form and the local heat flux increasing were related with this phenomenon. However, the detailed visualization by the shadow method did not show the hanging shock wave in the transition region [8, 9, 11]. Solutions of parabolized Navier-Stokes equations [10] revealed the presence of the intensive streamwise vortex near the wing symmetry plane, which was related with observed here extreme heat flux zone, but the mechanism of the heat exchange increasing was not clarified. It should be noted that the vortex was found also in solutions of Euler equations [11], and it was not understood, how the pure inviscid phenomenon related to the viscous effect of the surface heating. Under the middle span of the wing surface no flow structure

DOI: 10.13009/EUCASS2017-81

peculiarities was found and a reason of the appearance here regions with high heat fluxes and early laminar-turbulent transition retained not clear.

Solutions of full Navier-Stokes equations [12, 13] revealed the presence above the middle wing part the second intensive vortex (or two vortexes) with the streamwise orientation, which can be related with the formation the second zone of extreme heat exchange. The analysis of calculations allowed to relate the high heat flux spot appearance on the edge with the narrowing of the flow region between the shock wave and the leading edge forming due to the flow reconstruction from the explosive evolution to the swept leading edge flow regime. The comparison with experimental data of the calculated heat fluxes on the leading edge and all wing surface allowed to hope that the numerical method describes the considering flow well.

In this paper, the more detailed analysis the flow structure around the delta wing is presented on the base of numerical solutions of Navier-Stokes equations. The physical mechanism of the streamwise vortex formation under the middle wing part is directly related with the shape reconstruction of the bow shock wave near the nose. Effects of the vortex interaction with the boundary layer are analyzed. It allowed defining physical principals of the heat flux increasing and of the early laminar-turbulent transition.

In the second section, the problem formulation, methods of the numerical grid creation and the solution of equations using the code ANSYS CFX (the license of DAFWE MIPT) are outlined. In the third section, the flow structure near the leading edge in the vicinity of the wing nose is considered. In the fourth sections, results of the numerical modeling and its comparison with experimental data are presented for the main wing surface. In the fifth section the analysis of results is conducted. Basic conclusions are given in the final section. All calculations were performed using the DAFE MIPT cluster.

2. Problem formulation

In the present work, hypersonic flows at Mach numbers 6 -10.5, Reynolds numbers $(0.5 – 1.7)\cdot 10^6$ around delta wings with the leading edge sweep angle $\chi = 75°$, the bluntness radius of cylindrical edges and the spherical nose R = 3 and 8 mm, angles of attack $\alpha = 0°$ and 10° are considered under experimental conditions in the TsAGI wind tunnels UT-1M and T-117 [8, 12, 13]. The mathematical wing model and used Cartesian coordinate system with the origin in the centre of the nose bluntness are shown in Figure 1.

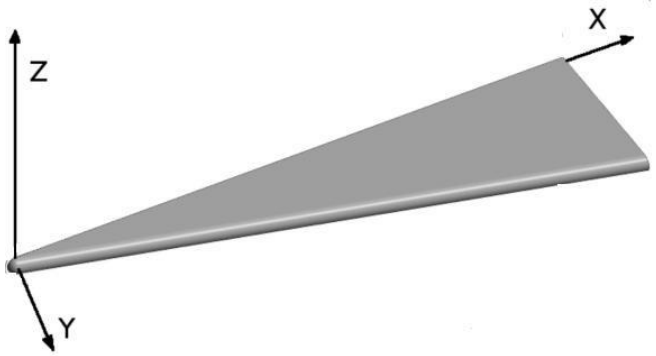

FIGURE 1. Figure 1: General view of the wing mathematical model

It is assumed the flow is described by full Navier-Stokes equations for the compressible, viscous and thermo-conducting, perfect gas with the viscosity defined by Sutherland formula. The wing surface is supposed to be isothermal with the temperature factor about 0.4 in correspondence with wind tunnel experiments; no-slip conditions are used for the flow velocities. Conditions on the left calculation region boundary corresponded to the homogeneous supersonic freestream. On the right boundary the flow was supersonic and soft conditions were put here; they have no influence to the flow in the calculation region. The flow is assumed to be symmetrical with respect to the plane $Y = 0$, and to reduce the computational resources only the half flow region is considered.

For the numerical approximation the finite-volume method and TVD-scheme with no increasing entropy and the limiter of Barth-Jespersen are used [14]. The realization of the code ANSYS CFX having the approximation accuracy of the second order in the space and of the first order in the time is used for calculations. The code ANSYS ICEM CFD is used to create geometrical and grid models. The calculation region dimension is selected so that the bow shock wave didn't cross the outer boundary. For calculations the unstructured hexagonal grid constructed using the block approach realized in the module HEXA is used. The grid model contained 7 blocks. To resolve dynamical

DOI: 10.13009/EUCASS2017-81

and temperature boundary layers and also large streamvise gradients of physical variables blocks with the minimal grid step been near the wing surface and its apex. The grid contained 170 cells in the orthogonal to the surface direction; the height of near-wall cells was fixed as 0.0015 mm. At least 10 cells were in the temperature boundary layer near the wing apex; about a quarter of all grid nodes were here and it ensures the well resolution.

Four grid models with 2, 4, 10 and 50 million nodes are used for the numerical calculations. The considered stationary problem was solved by the establishing method up to the discrepancy convergence. The maximum discrepancy for fluxes on the calculation region boundary was 10^{-6}, and inside the region it was 10^{-4}. The solution was found by several steps with the successive transition to finest grids. In the first step, the homogeneous freestream was used as the initial condition for calculation on the grid with 2 million nodes. This solution was used as the initial condition for calculations on the grid with 4 million nodes, which in the third step was the initial approximation for the grid with 10 million nodes. The final solution was obtained on the grid with 50 million nodes, and all presented results correspond to this grid. Such approach allows to reduce essentially the calculation time and to obtain the convergent solution.

3. The flow structure near the leading edge and local mechanism of heat flux increasing

In Figure 2, the qualitative picture of the heat flux distribution, $q = (\mu / \mathrm{Pr}) T_Z(X, Y, 0)$, on the leading edge and the windward surface of the wing model with the bluntness radius R = 8 mm at the angle of attack α = 10°, the Mach number M = 10.5 and the unit Reynolds number $\mathrm{Re}_1 = 4.1 \cdot 10^6$ m^{-1} is presented. Here μ is viscousity, Pr is Prandtl number, T is temperature. In this figure, two zones of increased heat fluxes on the leading edge and the main wing surface remote from the apex about on ten bluntness radii (10R) are exuded clearly. Reasons of their formation are different and are considered below.

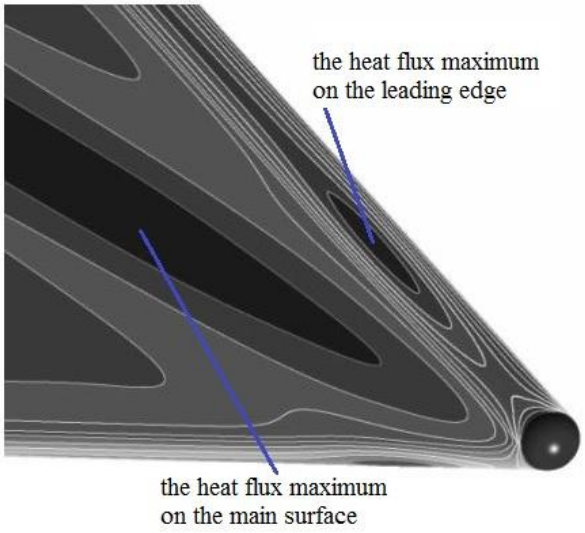

Figure 2: Heat flux density distribution on the leading edge and the windward surface of the wing

In Figure 3, the comparison of experimental (symbols) and computed (lines) heat flux density distributions referenced to the stagnation point heat flux q_0 along the attachment line on the wing leading edge at α = 10°, R = 8 mm for two flow conditions: M = 8.3 and $\mathrm{Re}_1 = 6.9 \cdot 10^6$ m^{-1} (the line 1) and M = 10.5, $\mathrm{Re}_1 = 4.1 \cdot 10^6$ m^{-1} (the line 2). The dotted line corresponds to the constant heat flux on the attachment line of the swept cylinder. It is seen calculation results agree well with experimental data in the TsAGI wind tunnel T-117 [8]. The heat flux maximum is at the distance about 10R from the apex.

Figure 4, in which for α = 10°, R = 8 mm, M = 8.3 and $\mathrm{Re}_1 = 6.9 \cdot 10^6$ m^{-1} the heat flux field on the windward wing surface and the flow static entropy field in the vicinity of the attachment line are presented, illustrates the physical mechanism of the heat flux increasing on the leading edge. The outer boundary of the dark region corresponds to the bow shock wave having the S-shaped form due to the bending in the transient region between the explosive flow regime near the wing nose and the flow of the swept cylinder type far enough from the apex [7, 10]. In the end of the

DOI: 10.13009/EUCASS2017-81

first zone before the bending the shock wave tilt angle is smaller than at the swept leading edge regime and here the flow after the shock wave has the smaller entropy and higher velocity directed to the leading edge. This flow presses to the surface the hot gas flowing from the near apex shock layer. In this location the flow region between the wing leading edge surface and the shock wave is narrowed that leads to reducing the velocity along the leading edge and to increasing of the velocity in the transverse direction. From the comparison Figure 4 with results in Fig. 3 it is seen that the leading edge heat flux maximum (it is the center of the light spot in Figure 4) corresponds to about the narrowest flow part and the minimum heat flux corresponds to about the widest flow part located upstream in the explosive flow zone. Similar results were obtained for the smaller bluntness radius R = 3 mm and at α = 0° at different Mach and Reynolds numbers.

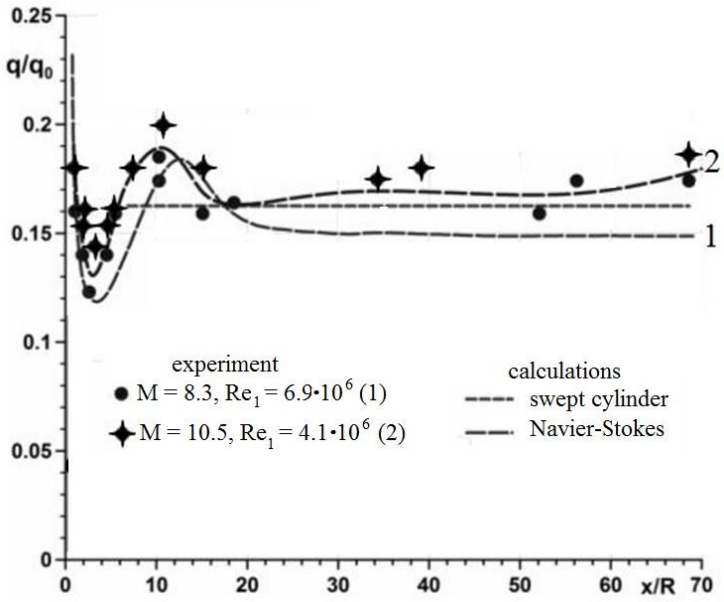

Figure 3: Heat flux density distribution on the leading wing edge attachment line

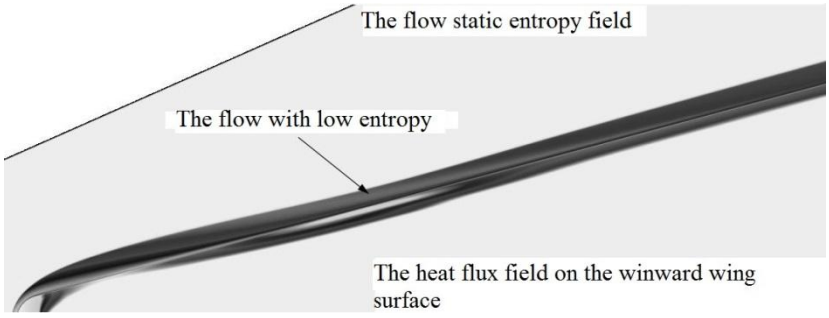

Figure 4: The flow static entropy field (the upper part) and the heat flux field on the windward surface near the leading edge (the lower part)

4. Perculiar properties of heat flux and laminar-turbulent transition over the main wing surface

Unusual properties of the heat exchange and the laminar-turbulent transition in the hypersonic boundary layer were found in wind tunnel experiments at the first on the surface of blunted half cones [2] and then on delta wings [3 – 9]. Specific heat flux distributions and limit streamlines on body surfaces are one of main results of hypersonic flow experimental investigations in wind tunnels, and they can be used for the numerical modeling verification. In the upper part of Figure 5, the calculated distribution of the specific heat flux on the wing surface at with the length 0.57 m, R = 8 mm at $\alpha = 0°$, the freestream Mack number M = 6, the unit Reynolds number $Re_1 = 1.1556 \cdot 10^6\ m^{-1}$, the total temperature $T_0 = 750$ K, the stagnation pressure $P_0 = 20$ atm are presented. The lower part of this figure corresponds to data obtained in the TsAGI shock wind tunnel UT-1M at about same conditions [8, 11, 13].

DOI: 10.13009/EUCASS2017-81

In the middle wing part, narrow streaks of the intensive heat exchange clearly identified as in calculations and experiments with the maximum specific heat flux q ≈ 8000-9000 Wt/m^2; this maximum depends mainly on Mach number and also the bluntness radius and Reynolds number. It should be noted in these streaks the heat flux increases to 3-4 times with respect to the background value that is compared with the laminar-turbulent transition effect and it can lead to unwanted consequences on real flying vehicles. In experiments these anomalies were known long enough [2] but reasons of their formation were not understand hitherto. As shown below, these anomalies relate with the quasistreamvise vortex, the axes of which are under streaks closer to the leading edge and follows to about the direction of its outer boundary.

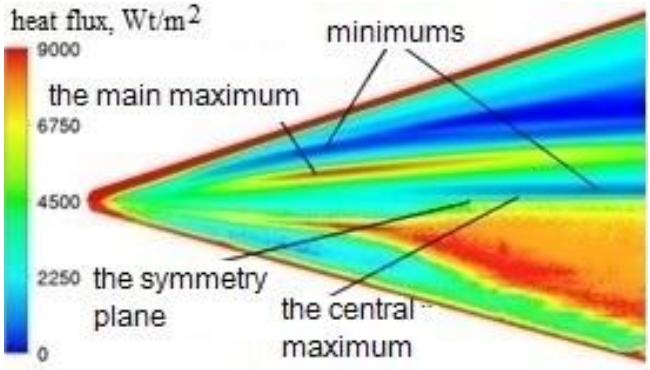

Figure 5: Comparison of numerical (the upper part) and experimental (the lower part) specific heat flux distribution on the wing surface.

Downstream, near the symmetry axis there is another higher heat exchange region with less values of the specific heat flux q ≤ 6750 Wt/m^2. It is shown below this anomaly is related with the elongated along the symmetry plane vortex; the location of this vortex with respect to the main vortex depends on flow parameters. The qualitative agreement of calculated and experimental distributions of the surface heat flux, at least up to the laminar-turbulent transition origin, allows hoping on the correct investigation possibility of considered flow structures using the numerical modeling.

In Figure 6 plots of the function $q(\bar{Y})$ at different cross-sections of the wing X = 0.12, 0.22, 0.32, 0.42, 0.52 m are presented. Along abscissa axes the dimensionless transverse coordinate $\bar{Y} = Y / b$ is measured, where $b(x)$ is the local half wideness of the wing. The maximum value of this function ($q_m \approx 8 \cdot 10^{-3}$) corresponds approximately to the point X_m = 0.2 m and $\bar{Y}_m$ = 0.4. This value exceed to 3-4 times the mean background value that compared with the growth of the heat flux in the laminar-turbulent transition. This circumstance does considered phenomenon very important in practical applications at large Mach numbers.

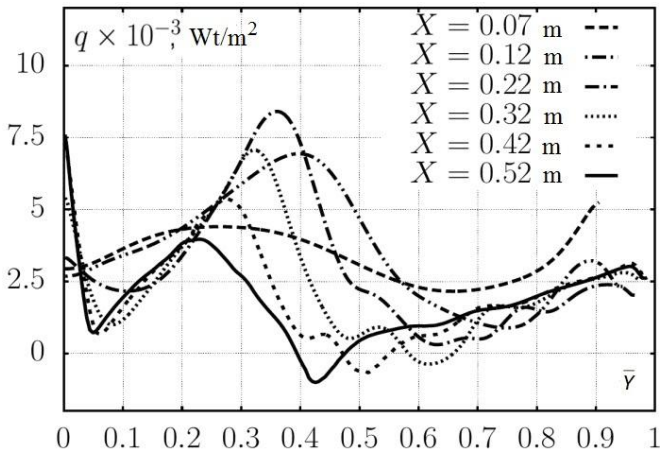

Figure 6: Specific heat flux $q(\bar{Y})$ distributions on the wing surface

DOI: 10.13009/EUCASS2017-81

Results in the lower part of Figure 5 show that in experiments the increased heat flux streak is expanded after reaching the maximum. This expansion is caused by the laminar-turbulent transition. It can notice the transition does not observed in regions located closer to the centerline and the leading edge, where its known transition mechanisms work: Tollmin-Schlichting or cross-flow instability. The given in Figure 5 transition observed in experiments on blunted wings and half-cones in hypersonic boundary layers only [2,3] and has a new type related exclusively with the evolving quasistreamwise vortex: this type has a smaller transition Reynolds number. The mechanism of this phenomenon is considered below.

5. Quasistreawise vortexes and effects of their interaction with the boundary layer

Considered above surface anomalies can be explained on the base of the analysis of the spatial flow structure, which is analyzed in details below for the case presented in Figures. 5 and 6. The general view of the flow structure in the cross-section X = 0.1 m after the formation in the apex vicinity of three vortexes with streamwise axes orientations is presented in Figure 7. This cross-section locates over the beginning of the heat-flux increasing wing surface region, which is shown in the lower half of the picture. The dark streak in the cross-section corresponds to the shock layer formed near the wing apex and containing the high entropy gas; the boundary layer is below it. It should be noted that in this section the gas temperature near the surface is essentially lower than in the shock layer.

The cross flow has the domed structure, the region of boundary and entropy layers expands in the direction to the symmetry plane that is related with the explosive character of the flow around the spherical nose in the hypersonic freestream. It is seen clear that in this cross-section three vortexes with approximately streamwise axes orientations have been formed already; the beginning of them formation locates in the wing apex vicinity. In the inviscid region above boundary and shock layers, the intensive clockwise rotating vortex has been formed; this vortex was found in solutions of Euler and parabolized Navier-Stokes equations [10, 11]. Its appearance is determined by the entropy layer thickening to the symmetry plane, i.e. by its domed shape and related with this inviscid effect the flow retardation in this direction.

Inside the boundary layer there are two counterclockwise rotating vortexes, which were found in Navier-Stokes equations solutions only. The central vortex locates directly near the symmetry plane; its formation defined by the requirement of satisfying symmetry conditions inside the boundary layer, equations of which have the singularity in the delta wing symmetry plane [15]. The intensity of this vortex is small and the heat flux increase under it is slight.

The second (main) vortex locates in the middle span part of the wing. The analysis of calculation results shown that this vortex is formed at the distance approximately 0.078 m (about 10 bluntness radii) from the wing apex under two opposite trends: 1) the growth of the cross velocity directed to the symmetry plane in the inviscid narrowing flow region between the shock wave the leading edge; 2) the viscous flow of the opposite direction in the near-wall boundary-layer region defined by the induced by viscous-inviscid interaction cross-flow pressure gradient. Due to the boundary layer thickness growth and the diffusive absorption of the shock layer by the viscous flow these two regions with opposite velocities are converged, and at $X \geq 0.07$ m due to them interaction the rotated flow is formed.

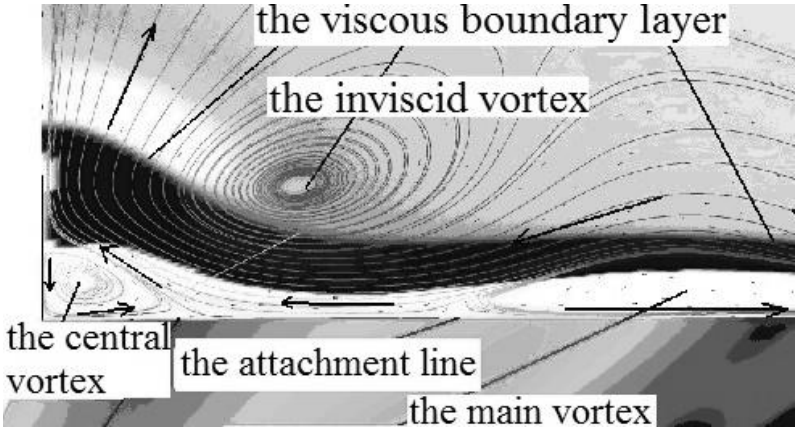

Figure 7: The flow structure above the wing surface in the cross-section X = 0.1 m

DOI: 10.13009/EUCASS2017-81

The flow structure can vary in dependence of the curvature radius, Mach and Reynolds numbers [8, 12]. The central vortex can be located upstream or downstream with respect to the main vortex or can't arise. At large Mach numbers the middle flow region can contain two vortexes of opposite rotations but not the one vortex as in Figure 7 [12].

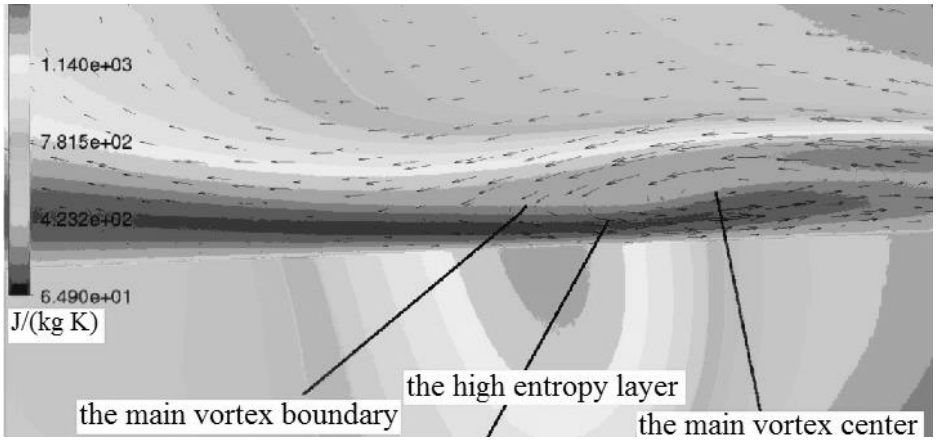

Figure 8: Streamlines and the entropy distribution in the cross-section X = 0.2 m above the heat flux maximum on the wing

In the upper part of Figure 8, cross-flow streamlines and the entropy distribution in the section X = 0.2 m approximately corresponding to the specific surface heat flux maximum are presented; in the low part of Figure 8 the heat flux distribution on the wing is shown. It is followed from these data, specific heat flux distributions on Fig. 6 and the cross skin friction distributions $\tau_y\left(\bar{Y}\right)$ in Figure 9 the attachment line formed by the vortex (the cross-flow stagnation point, $\tau_y = 0$) locates at the edge ($\bar{Y} \approx 0.22$) of the intensive heat exchange region, but the heat flux maximum corresponds to $\bar{Y} \approx 0.37$ in the section X = 0.2 m; the vortex center locates under the point $\bar{Y} \approx 0.43$ that corresponds to the maximum of the function $\tau_y\left(\bar{Y}\right)$. It can see that in contrast to section of the increasing heat flux region beginning at X = 0.1 m (Figure 7), in this section the highest entropy gas (the dark region) locates in the near-wall layer closest to the surface under the maximum heat flux point.

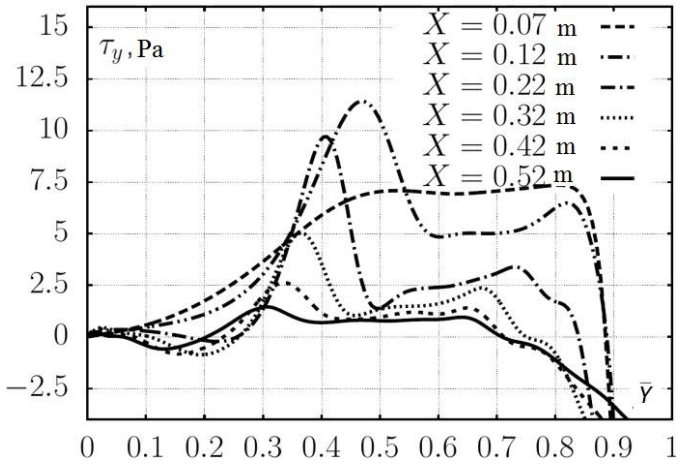

Figure 9: Transverse skin friction $\tau_y\left(\bar{Y}\right)$ distributions on the wing surface

In Figure 10 profiles of transverse ($W\left(\bar{Z}\right)$, Figure 10a) and streamwise ($U\left(\bar{Z}\right)$,Figure 10b) velocities along the vortex axis are presented. In these plots, the dimensionless normal to the wing surface coordinate $\bar{Z} = Z / \Delta$ referenced to the local boundary layer thickness Δ is measured along ordinate axes. These results demonstrate that the section of the maximum heat exchange ($X \approx$ 0.2 m) corresponds to the most vortex intensity (the cross-flow velocity maximum) and maximal transverse and streamwise shear stresses. Maximal cross-flow skin friction values on the wall at sections (Fig. 8) are achieved under the vortex axis. After the vortex formation in the section $X \approx$

DOI: 10.13009/EUCASS2017-81

0,078 m, its intensity growths downstream that indicates the cross-flow profiles (Figure 10a), and achieves to the maximum value in the section $X \approx 0.2$ m corresponding to the maximal surface heat exchange. The comparison of transverse and streamwise velocity profiles also shows that the vortex region in two times thicker than the boundary layer if the edge of it is defined by streamwise velocity or temperature distributions.

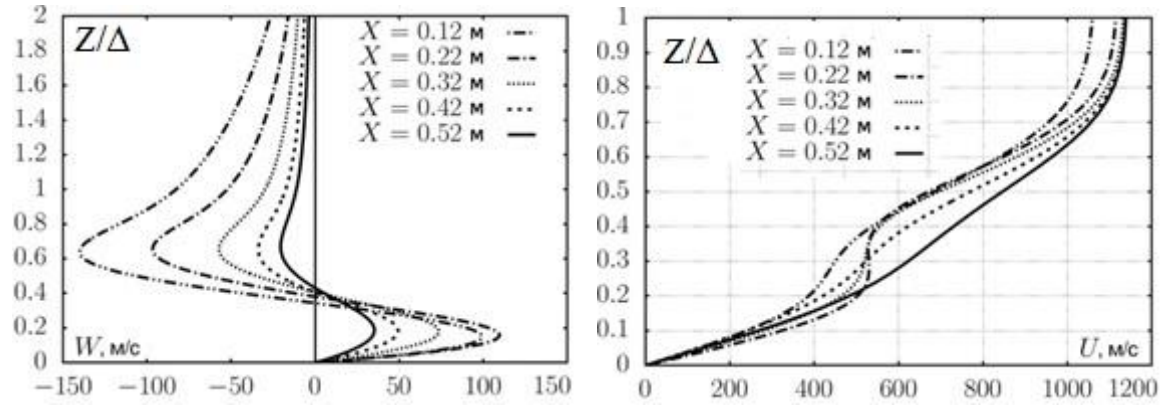

a) b)

Figure 10: Profiles of transverse (a) and longitudinal (b) velocity components along the main vortex axis

In the section $X \approx 0.2$ m, the streamwise velocity profile becomes fully flat at the vortex axis (Figure 10b), and the cross-flow velocity near the wall achieves to the maximum $W \approx 110$ m/s, which about in 10 times less of the streamwise velocity. Downstream this section, the vortex weakens, the cross-flow velocity decreases and the streamwise velocity profile become more full but the inflectional point does not disappears that is very important circumstance for understanding the formed physical flow structure. It was noted above in the experiment (the lower half of Figure 5) after epy achievement of the maximum vortex intensity the laminar-turbulent transition is developed.

It should be noted the change of the heat flux larger than to three times, as its distributions in Figure 6, show, can't be explained by the deceleration of the cross-flow. The enthalpy h and the temperature T in the near-wall boundary-layer region and also them normal derivatives at the wall can define by relations:

$$h = c_p T = H_0 - \frac{1}{2}\left(U^2 + W^2 + V^2\right); \quad h_Z\left(X,Y,Z\right) = H_{0Z}\left(X,Y,Z\right)$$

It is followed from the second formula the heat flux directly relates with of the total enthalpy derivative H_{0Z}. On the wing surface flow velocities are zero and they don't influence to the heat flux. The normal velocity V in the boundary layer to an order less than the transverse velocity W, which in turn to ten times less than the streamwise velocity U. So, variation of transverse and normal velocity can change the enthalpy on few percent only. It means the temperature distribution in the boundary layer is defined mainly by the streamwise velocity.

Commonly the Reynolds analogy, which is relating linearly heat flux with the streamwise skin friction, is used for heat flux estimations. In the considered case, the largest streamwise velocity deformation and the growth of its derivative happen under the vortex axis and on its periphery essentially weaken (see Fig. 10b). Then, if the hypothesis about the similarity of streamwise skin friction and heat flux distributions would be true, the maximum heat flux will be observed along the vortex axis. However, in calculations it arises between locations of the axis and the cross-flow attachment line.

The detailed analysis of the spatial flow structure showed that in initial moments of the vortex formation the hottest gas is in the shock layer above the boundary layer, as it shown in Fig. 6. The vortex captures this hot gas and in the downward evolution process transfers it to the surface during the half turnover around the axis that is demonstrated in the figure 7. Inside the vortex, right from the attachment line the hot gas is pressed to the wall, where the higher heat flux region is formed. Left from the attachment line the vertical velocity is positive, the flow is directed to the outer boundary layer edge and the heat flux don't increase here. Therefore, the appearance of the extreme heat flux zone is defined by the convective vortex transfer to the wing surface of the hot gas with the increased full enthalpy

DOI: 10.13009/EUCASS2017-81

from the shock layer located after the about direct shock wave before the nose. This conclusion is agreed also with the presented above relation for enthalpy derivatives, from which is followed that on the wall $T_z \sim H_{0z}$, i.e. the heat flux change is directly relates with increasing of the total local enthalpy.

Another result of the vortex-boundary layer interaction is the formation inside the later the velocity profile like to that of inside the twisted jet or the vortex in the cocurrent freestream. The velocity profile inside the boundary layer has the inflection point and even became flat near the vortex intensity maximum ($X \approx 0.2$ m). Such velocity profile is unstable with respect to Rayleigh mode that is provoked the essentially earlier laminar-turbulent transition, than Tollmen-Schlichting waves [16]. On the other hand, the cross-flow velocity profile has the S-shaped form along the vortex axis that leads to the excitation of the cross-flow instability waves, which also lead to earlier transition [16]. The observed in experiments phenomenon (the lower part of Fig. 5) very reminds one of the laminar vortex break scenario, defined by the development inside it unstable disturbances and the transition to the turbulence. What is transition mechanism at each concrete set of parameters – Rayleigh or cross-flow instability – can be defined as a result of the considered flow hydrodynamic stability analysis that is out of these frameworks.

6. Conclusions

On the base of experimental data and the numerical modeling using the code complex ICEM CFX the structure of hypersonic viscous gas flows around of the delta wing with blunted leading edges is studied. Computed heat flux surface distributions agree satisfactory with experimental data that is verified the used method.

Found experimentally streaks of the higher heat flux near the symmetry plane and in the middle part of the wing surface are defined by formations of nearly streamwise vortex structures. These vortexes have different formation mechanisms: the vortex near the symmetry plane is defined by the retardation conditions; the main vortex forms by the increasing of the outer cross-flow intensity in the transient region from the nose explosive flow type to flow around the swept leading edge and the viscous-inviscid interaction. These vortexes are obtained by the numerical modeling on the base of full Navier-Stokes equations only. In solutions of Euler and parabolized Navier-Stokes equations they cannot realize; obtained in these solutions vortexes have pure inviscid origin.

Presented results show that in the contrary to two-dimensional flows, where the interaction of shock and boundary layers is defined by the diffusive absorption of the first only, in spatial flows the streamwise vortex can formed and they can convectively transfer the hot gas from the shock layer into the near-wall boundary-layer region. This process leads to the appearance of higher heat flux zones on the wing surface.

The second effect of the vortex and the boundary layer interaction leads to the inflection point formation on the streamwise velocity profile and to the development of Rayleigh instability. The cross-flow velocity profile along the vortex axis has S-shaped form that leads to the excitation of the cross-flow instability. Both these phenomena lead to the earlier laminar-turbulent transition appearance and to the vortex breaking that explains experimentally observed phenomena.

Acknowledgments

This work was performed at the RFBR support by the grant N 15-01-03615.

References

[1] V.Ya. Neyland, V.V. Bogolepov, G.N. Dudin, I.I. Lipatov. 2004. Asymptotic theory of supersonic viscous gas flows (Fizmatlit, Moscow)..

[2] V.Ya. Borovoi, R.Z. Davlet-Kildeev M.V. Ryzhkova. 1968. On heat exchange peculiarities on the surface of some lifting bodies at large supersonic speeds. *Izvestia RAN, MZhG*: 1

[3] I.A. Kondratiev, A.Ya. Yushin, 1990. On local heat flux increasing on the windward surface of a delta wing with blunted leading edges. Aerothermodynamics of aerospace systems, Report collection of TsAGI school-seminar “Mechanics of liquid and gas. TsAGI, Zhukovsky. 1: 167–175.

[4] O.I. Gubanova, B.A. Zemlyansky, A.B. Lesin, V.V. Lunev, A.N. Nikulin, A.V. Syusin, 1990. Abnormal heat exchange on the winward side of the delta wing with the blunted nose at hypersonic speeds. Aerothermodynamics of aerospace systems, Report collection of TsAGI school-seminar “Mechanics of liquid and gas. TsAGI, Zhukovsky. 1: 188–196.

DOI: 10.13009/EUCASS2017-81

[5] N.A. Kovaleva, N.P. Kolina, A.Ya. Yushin. 1993. Experimental investigations of the heat exchange and the laminar-turbulent transition on delta half-wing models in supersonic flows. Uchenye zapiski TsAGI. XXIV, N 3: 46–52.
[6] A.B. Lesin, V.V. Lunev. 1994. On peak heat fluxes on the triangular plate with the blunted nose. Izvestia RAN, MZhG. 2: 131–137.
[7] V.V. Lunev. 2007. Flows of real gases with high speeds. Physmathlit, Moscow.
[8] V.N. Bragko, A.V. Vaganov, G.N. Dudin, N.A. Kovaleva, I.I. Lipatov, A.S. Skuratov. 2009. Experimental investigation of aerodynamic heating peculiarities at large Mach numbers. Proceedings of MIPT 1, N 3: 57–66.
[9] A.V. Vaganov, Yu.G. Yermolaev, A.D. Kosinov, N.V. Semenov, V.I. Shalaev. 2013. Experimental investigation of the flow structure and the transition in the boundary layer on the delta wing with blunted leading edges at Mach numbers Maxa 2, 2,5 and 4. *Proceedings of MIPT*. 5, N 3(19): 164-173.
[10] V.I. Vlasov, A.B. Gorshkov, R.V. Kovalev, V.V. Lunev. 2009. A thin triangular plate with the blunted nose in the viscous hypersonic flow. *Izvestia RAN, MZhG*. 4: 134–145.
[11] V.N. Bragko, A.V. Vaganov, V.E. Mosharov, V.N. Radchenko, S.V. Chernov. 2011. Calculated-experimental investigation of the flow structure over the windward surface of the delta blunted wing. Materials of XIV International school-seminar "Models and methods of aerodynamics". MTsNMO, Moscow: 28-29.
[12] V.N. Bragko, A.V. Vaganov, V.Ya. Neyland, M.A. Starodubtsev, V.I. Shalaev. 2013. Modeling of flow pecularities on the windward delta wing side with with blunted leading edges on the base of the Navier-Stokes numerical solution. *Proceedings of MIPT*. 5, N 2 (18): 13-22.
[13] S.V. Aleksandrov, A.V. Vaganov, V.I. Shalaev. 2016. Physical Mechanisms of Longitudinal Vortexes Formation, Appearance of Zones with High Heat Fluxes and Early Transition in Hypersonic Flow over Delta Wing with Blunted Leading Edges. International Conference on the Methods of Aerophysical Research, AIP Conf. Proc. 1770, 020011-1–020011-10; doi: 10.1063/1.4963934.
[14] Barth T. J., Jespersen D. C. 1989. The design and application of upwind schemes on unstructured meshes. *AIAA paper* 89-0366.
[15] V.I. Shalaev. 2010. Application of analytical methods in modern aeromechanics. Part 1. Boundary layer theory. MIPT, Moscow. 300 p.
[16] W.S. Saric, H.L. Reed, E.B. White. 2003. Stability and transition of three-dimensional boundary layers. *Annual Review of Fluid Mechanics* 35: 413–440.